Effect of past stretching sheet with constant wall temperature Under the heat transfer flow on nano fluids by using Legendre Wavelet Method

[1]Sangeeta Sharma and [2]Dr. Sandeep Kumar Tiwari
[1]Research Scholar, Motherhood University, Roorkee
[2]Department of Mathematics, Motherhood University, Roorkee
Email: [1]Sonu21.bhawna@gmail.com **and** [2]Sandeepbsm2012@gmail.com

Abstract: This study analyses the effect of partial slip boundary conditions on the boundary-layer flow and heat transfer of nanofluids over a stretching sheet exposed to a constant wall temperature. The nanofluid model accounts for Brownian motion and thermophoresis effects, which are crucial in modelling the dynamics of nanoparticle transport. Through classical similarity transformations, the governing conservation equations are reduced to a coupled system of nonlinear ordinary differential equations. However previously used numerical approaches, the present work uses the Legendre Wavelet Method (LWM) as an efficient and correct semi-analytical technique for solving the transformed equations. The impacts of key dimensionless parameters— including the slip factor, Brownian motion parameter, Prandtl number, Lewis number and thermophoresis parameter—on the temperature, velocity and nanoparticle concentration fields are examined in detail. The results shows that the slip boundary condition substantially changes the flow structure, surface shear stress, reduced Nusselt number, and reduced Sherwood number. To the best of the authors' knowledge, this study represents the first application of Legendre wavelets to nanofluid slip-flow problems include the dynamic effects of nanoparticles over a stretching sheet.

[Sharma, S. and Tiwari, S.K**. Effect of past stretching sheet with constant wall temperature Under the heat transfer flow on nano fluids by using Legendre Wavelet Method.** *The International Journal of Interpretation, Observation and Analysis*, 2025; Volume 4, Issue 1:164-172 (October-December). ISSN 2349-0713, Peer-reviewed (online/offline), Refereed, Indexed and International Journal (Since 2013), Global Impact Factor: 6.205

Keywords: Nanofluid, Legendre wavelet Method, Boundary layer flow, Stretching sheet, Similarity transformation Thermophoresis, Heat and mass transfer, Partial slip boundary condition, Constant wall temperature, Brownian motion

Introduction: Nanofluids, defined as dispersion of solid nanoparticles with characteristic length scales of 1–100 nm dispersed in conventional heat-transfer base fluids, have attracted important research interest due to their enhanced thermophysical properties. The inclusion of nanoparticles markedly improves the thermal conductivity and convective heat-transfer coefficient of base fluids such as water, oil, and ethylene glycol, which otherwise exhibit relatively poor heat-transfer performance. To overcome these limitations, numerous techniques have been developed in recent decades to increase heat-transport efficiency, among which the addition of nanoparticles has proven particularly effective [1]. Choi et al. [3] first demonstrated that nanoparticle dispersion can nearly double the thermal conductivity of conventional fluids, motivating extensive studies on the thermophysical behaviour of nanofluids, including the work of Khanafer et al. [4] and others.

Nanotechnology's immediate development has further amplified interest in modelling nanofluid transport phenomena, especially within boundary-layer regimes of industrial significance. Flow and heat transfer over stretching sheets constitute a classical problem in fluid mechanics and arise in many engineering applications such as polymer extrusion, metal processing, glass blowing, and film drawing [5–10]. The thermal performance of the cooling or heating fluid plays a conclusive role in determining product quality in these processes [11]. Since Crane's seminal work [5], boundary-layer flow over stretching surfaces has been comprehensively examined under diverse physical effects, including suction and injection [12], magnetic fields [13], variable thermal boundary conditions [14], micropolar effects [15], nanofluid behaviour [16], and non-Newtonian rheology [17,18]. Despite substantial progress, the governing equations describing nanofluid flow with slip at the stretching surface are highly nonlinear and strongly coupled, making them challenging to solve using conventional analytical or numerical techniques. There remains a need for stable computational approaches capable of delivering accurate, rapidly convergent solutions for such boundary-layer problems. To address this gap, the present study employs the Legendre Wavelet Method (LWM) to investigate the effects of slip boundary conditions on nanofluid flow and heat transfer over a stretching sheet. The LWM offers significant advantages due to its orthogonal basis functions, multiresolution structure, and strong capability in approximating nonlinear differential equations with high accuracy and low computational cost. These features make the method specifically suitable for boundary-layer models characterized by steep gradients and complex interactions among

velocity, thermal, and nanoparticle concentration fields. The objective of this work is therefore to provide a comprehensive analysis of slip-induced heat-transfer characteristics in nano fluid flow over a stretching sheet using the Legendre Wavelet Method. The results presented here in contribute to the development of optimal solution techniques and offer improved physical insight into thermally improved nanofluid systems pertinent to contemporary industrial processes.

Governing equation

Consider a steady, two-dimensional, incompressible viscous flow of a nanofluid over a stretching surface. The surface is stretched linearly in the x-direction with a velocity

$$U_w(x) = cx,$$

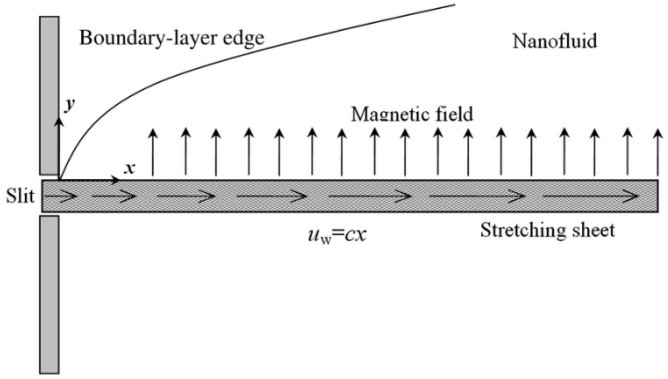

where c is a positive constant and x is the coordinate measured along the sheet. The coordinate system and schematic of the physical configuration are shown in fig. The flow develops along the stretching surface located at $y = 0$, where y denotes the coordinate normal to the surface. The temperature and nanoparticle volume fraction at the wall are prescribed as constant values T_w and ϕ_w, respectively. Far from the surface ($y \to \infty$), the fluid approaches the ambient temperature T_∞ and nanoparticle volume fraction ϕ_∞. Brownian motion and thermophoresis effects are assumed to be significant in the near-wall region, as is typical in laminar nanofluid boundary layers. Under these assumptions, the governing steady, two-dimensional conservation equations for mass, momentum, thermal energy, and nanoparticle concentration in Cartesian coordinates (x, y)take the following forms:

Continuity equation

$$\frac{\partial u}{\partial x} + \frac{\partial v}{\partial y} = 0, \qquad (1)$$

Momentum equations

$$u\frac{\partial u}{\partial x} + v\frac{\partial u}{\partial y} = -\frac{1}{\rho_f}\frac{\partial p}{\partial x} + \nu\left(\frac{\partial^2 u}{\partial x^2} + \frac{\partial^2 u}{\partial y^2}\right), \qquad (2)$$

$$u\frac{\partial v}{\partial x} + v\frac{\partial v}{\partial y} = -\frac{1}{\rho_f}\frac{\partial p}{\partial y} + \nu\left(\frac{\partial^2 v}{\partial x^2} + \frac{\partial^2 v}{\partial y^2}\right), \qquad (3)$$

Energy equation

$$u\frac{\partial T}{\partial x} + v\frac{\partial T}{\partial y} = \alpha\left(\frac{\partial^2 T}{\partial x^2} + \frac{\partial^2 T}{\partial y^2}\right) + \sigma\left[D_B\left(\frac{\partial \phi}{\partial x}\frac{\partial T}{\partial x} + \frac{\partial \phi}{\partial y}\frac{\partial T}{\partial y}\right) + \frac{D_T}{T_\infty}\left(\left(\frac{\partial T}{\partial x}\right)^2 + \left(\frac{\partial T}{\partial y}\right)^2\right)\right], \qquad (4)$$

Nanoparticle concentration equation

$$u\frac{\partial \phi}{\partial x} + v\frac{\partial \phi}{\partial y} = D_B\left(\frac{\partial^2 \phi}{\partial x^2} + \frac{\partial^2 \phi}{\partial y^2}\right) + \frac{D_T}{T_\infty}\left(\frac{\partial^2 T}{\partial x^2} + \frac{\partial^2 T}{\partial y^2}\right). \qquad (5)$$

Here,

u and $v$are the velocity components along $x$and y;

p is the fluid pressure;

$\sigma = (\rho c_p)_p/(\rho c_p)_f$is the ratio of nanoparticle heat capacity to that of the base fluid;

ρ_f is the density of the base fluid;

ν and α denote the kinematic viscosity and thermal diffusivity,

D_B is the Brownian diffusion coefficient;

D_T is the thermophoretic diffusion coefficient;
and ϕ represents the nanoparticle volume fraction.

Boundary Conditions

The boundary conditions at the stretching surface $y = 0$ incorporate a velocity slip following Navier's model:

$$v = 0, u = U_w(x) - U_s, T = T_w, \phi = \phi_w, \qquad (6)$$

where U_s denotes the slip velocity at the wall, assumed proportional to the local shear stress.
The far-field boundary conditions ($y \to \infty$)are given by

$$u \to 0, v \to 0, T \to T_\infty, \phi \to \phi_\infty. \qquad (7)$$

To obtain similarity solutions of Equation (1)– (5), we introduce the stream function ψ and the following dimensionless similarity variables:

$$\psi = (cv)^{1/2}\, x\, f(\eta), \eta = (\frac{c}{v})^{1/2} y, \qquad (8a)$$

$$\theta(\eta) = \frac{T - T_\infty}{T_w - T_\infty}, \emptyset(\eta) = \frac{\phi - \phi_\infty}{\phi_w - \phi_\infty}, \qquad (8b)$$

where, $\theta(\eta)$is the nondimensional temperature, $f(\eta)$is the dimensionless stream function and $\emptyset(\eta)$denotes the nondimensional nanoparticle concentration.

The velocity components automatically satisfy the continuity equation (1) by defining

$$u = \frac{\partial \psi}{\partial y} = U_w(x)\, f'(\eta), v = -\frac{\partial \psi}{\partial x} = -(cv)^{1/2} f(\eta),$$

where $U_w(x) = cx$ is the stretching velocity. Thus, the reduced axial velocity becomes $f'(\eta) = u/U_w(x)$.
Since the flow is driven solely by the stretching sheet and no external pressure gradient is imposed, the pressure field outside the boundary layer becomes constant. Consequently, the pressure gradient term in the boundary-layer momentum equation can be neglected. Substituting the similarity transformations (8a–b) into Equation (2)– (5) and applying standard boundary-layer approximations yield the following system of ordinary differential equations

Momentum equation

$$f''' + ff'' - (f')^2 = 0, \qquad (9)$$

Energy equation

$$\frac{1}{Pr}\, \theta'' + f\theta' + Nb\, \phi'\theta' + Nt\, (\theta')^2 = 0, \qquad (10)$$

Nanoparticle concentration equation

$$\emptyset'' + \frac{Nt}{Nb}\theta'' + Le\, f\phi' = 0, \qquad (11)$$

Where

$$Pr = \frac{\nu}{\alpha} \text{(Prandtl number)},$$

$$Nb = \frac{\tau D_B(\phi_w - \phi_\infty)}{\nu} \text{(Brownian motion parameter)},$$

$$Nt = \frac{\tau D_T(T_w - T_\infty)}{\nu T_\infty} \text{(thermophoresis parameter)},$$

$$Le = \frac{\nu}{D_B} \text{(Lewis number)},$$

and
$\tau = (\rho c_p)_p/(\rho c_p)_f$is the nanoparticle heat capacity ratio

Transformed Boundary Conditions

Introducing Navier's slip condition at the wall, the boundary conditions (6)– (7) transform into:

$$f(0) = 0, f'(0) = 1 - \lambda f''(0), \theta(0) = 1, \beta(0) = 1, \quad (12)$$

$$f'(\eta) \to 0, \theta(\eta) \to 0, \beta(\eta) \to 0 \text{as } \eta \to \infty, \quad (13)$$

where λ is the dimensionless slip parameter defined by

$$\lambda = \frac{U_s}{(c\nu)^{1/2}}.$$

By applying the similarity transformations defined in Equation (8a)–(8b) to the wall slip condition, the slip boundary condition (12) reduces to

$$f'(0) - 1 = \lambda f''(0), \quad (13)$$

Where

$$\lambda = N_r(\frac{c}{\nu})^{1/2}$$

is the dimensionless slip factor.

Equations (9)– (11) constitute a coupled, nonlinear boundary-value problem that can be solved subject to the following boundary conditions:

At the wall $\eta = 0$:

$$f(0) = 0, f'(0) = 1 + \lambda f''(0), \theta(0) = 1, \beta(0) = 1, \quad (14)$$

As $\eta \to \infty$:

$$f'(\eta) \to 0, \theta(\eta) \to 0, \beta(\eta) \to 0. \quad (15)$$

Here, primes denote differentiation with respect to η. The dimensionless parameters appearing in Eqs. (9)– (11) are defined as

$$Pr = \frac{\nu}{\alpha}, Le = \frac{\nu}{D_B}, \quad (16a)$$

$$Nb = \frac{(\rho c_p)_p D_B(\phi_w - \phi_\infty)}{(\rho c_p)_f \nu}, Nt = \frac{(\rho c_p)_p D_T(T_w - T_\infty)}{(\rho c_p)_f \nu T_\infty}, \quad (16b)$$

where Pr is the Prandtl number, Le is the Lewis number, Nb the Brownian motion parameter, and Nt the thermophoresis parameter. In continuum modelling, a no-slip condition is traditionally assumed for Newtonian fluids. However, for nanofluids, this assumption may not be valid because the presence of nanoparticles often generates partial slip at the solid boundary. Experimental and theoretical studies indicate that nanofluid flows commonly to show finite tangential slip, which may be characterized by a slip length ranging from approximately 3.4–68 nm for a wide range of liquids. Most nanofluids studied in the literature exhibit Lewis numbers $Le > 1$ [39]. For water-based nanofluids at room temperature containing nanoparticles with diameters of 1–100 nm, the Brownian diffusion coefficient $D_B$typically lies in the range 4×10^{-4} to 4×10^{-12} m ^{2}/s [38]. Moreover, the ratio of Brownian diffusivity to thermophoretic diffusivity varies between 2–0.02 for alumina nanoparticles and 2–20 for copper nanoparticles. Based on earlier studies by Khan and Pop, Rana and Bhargava, and Makinde and Aziz, the parameters Nb and Nt are commonly examined in the range 0.1–0.5 , with Lewis numbers typically between 1–25 . Accordingly, the present study considers parameter variations within these physically realistic ranges. When $Nb = Nt = 0$, Eqs. (10)– (11) reduce to the classical problem of viscous boundary-layer flow and heat transfer over a stretching surface. In such a limiting case, the equation governing β becomes ill-posed due to the absence of nanoparticle transport mechanisms.

Heat and Mass Transfer Characteristics

The local Nusselt number Nu_x and Sherwood number Sh_x, which characterize the rates of heat and mass transfer at the stretching sheet, are defined as

$$Nu_x = \frac{x\, q_w}{k(T_w - T_\infty)}, Sh_x = \frac{x\, q_m}{D_B(\phi_w - \phi_\infty)}, \qquad (17)$$

where q_w and q_m denote the wall heat and mass fluxes, respectively.

Using the similarity transformations (8a)–(8b), these expressions simplify to the reduced Nusselt and Sherwood numbers:

$$Re_x^{1/2} Nu_x = -\theta'(0), Re_x^{1/2} Sh_x = -\beta'(0), \qquad (18)$$

Where

$$Re_x = \frac{U_w(x)x}{\nu}$$

is the local Reynolds number based on the stretching velocity $U_w(x)$. Kuznetsov and Nield [20] referred to $Re_x^{1/2} Nu_x$ and $Re_x^{1/2} Sh_x$ as the *reduced* Nusselt and Sherwood numbers, respectively—a convention also used by Khan and Pop [32].It is worth noting that Andersson [42] and Wang [29] obtained exact solutions of Eq. (9) for the case of viscous flow over a stretching sheet with boundary conditions corresponding to Equation. (14)– (15). Their results serve as important benchmarks for validating numerical or semi-analytical techniques applied to this class of boundary-layer flows.

Numerical method

Let $P_m(\xi)$ be the Legendre polynomial of order m defined on $\xi \in [-1,1]$. Using a linear mapping from $\eta \in [0,\infty)$to a finite computational domain $\xi \in [-1,1]$, the Legendre wavelets of order k and resolution level $J$are defined as:

$$\psi_{m,j}(\eta) = \begin{cases} 2^{j/2} P_m(2^j \eta - l), & \eta \in [\frac{l}{2^j}, \frac{l+1}{2^j}], \\ 0, & \text{otherwise}, \end{cases}$$

where $j = 0,1,\dots,J-1$, $m = 0,1,\dots,k-1$, and $l = 0,1,\dots,2^j - 1$.

These wavelets form an orthonormal basis in $L^2([0,1])$, to make possible the representation of unknown functions and their derivatives.

Wavelet Expansion of the Unknown Functions

The similarity functions $f(\eta)$, $\theta(\eta)$, and $\phi(\eta)$are approximated as finite Legendre-wavelet series:

$$f(\eta) \approx \sum_{i=1}^{M} a_i\, \psi_i(\eta), \theta(\eta) \approx \sum_{i=1}^{M} c_i\, \psi_i(\eta), \phi(\eta) \approx \sum_{i=1}^{M} d_i\, \psi_i(\eta), \qquad (19)$$

where $M = k2^J$ denotes the total number of basis functions. Because the governing equations include up to the third derivative of f, derivatives of the wavelet expansions are obtained analytically:

$$f'(\eta) = \sum a_i \psi_i'(\eta), f''(\eta) = \sum a_i \psi_i''(\eta), f'''(\eta) = \sum a_i \psi_i'''(\eta). \qquad (20)$$

The derivative matrices $D^{(1)}, D^{(2)}, D^{(3)}$are prepared once and remain constant for all computations, resulting in a highly efficient formulation.

Reduction of Governing Equations to an Algebraic System

Substituting the wavelet expansions into Equation. (9)– (11):

$$f''' + ff'' - (f')^2 = 0,$$
$$\frac{1}{Pr}\theta'' + f\theta' + Nb\phi'\theta' + Nt(\theta')^2 = 0,$$
$$\phi'' + \frac{Nt}{Nb}\theta'' + Le\, f\phi' = 0,$$

yields a system of nonlinear algebraic equations in terms of the coefficients a_i, c_i, d_i for $i = 1,2, \dots, M$.

Collocating the residuals at Gauss–Legendre nodes $\{\eta_j\}_{j=1}^{M}$ gives:

$$R_f(\eta_j) = 0, R_\theta(\eta_j) = 0, R_\phi(\eta_j) = 0$$

for all $j = 1, \dots, M$.

This produces $3M$ nonlinear algebraic equations.

Imposition of Boundary Conditions

The boundary conditions (14)– (15):

$$f(0) = 0, f'(0) = 1 + \lambda f''(0), \theta(0) = 1, \phi(0) = 1,$$
$$f'(\infty) = 0, \theta(\infty) = 0, \phi(\infty) = 0,$$

are imposed by replacing rows of the algebraic system with:

$$\sum a_i \psi_i(0) = 0,$$
$$\sum c_i \psi_i(0) = 1, \sum d_i \psi_i(0) = 1,$$
$$\sum a_i \psi_i'(\eta_\infty) = 0, \sum c_i \psi_i(\eta_\infty) = 0, \sum d_i \psi_i(\eta_\infty) = 0,$$

where η_∞ is chosen sufficiently large (typically 6–10).

Calculation of Physical Quantities

After recovering the coefficient vectors $A = \{a_i\}, C = \{c_i\}, D = \{d_i\}$, the reduced Nusselt and Sherwood numbers follow directly from:

$$\mathrm{Re}_x^{-1/2} Nu = -\theta'(0), \mathrm{Re}_x^{-1/2} Sh = -\phi'(0),$$

where derivatives at the wall are computed from the wavelet derivative matrices:

$$\theta'(0) = \sum c_i \psi_i'(0), \phi'(0) = \sum d_i \psi_i'(0).$$

Results and Discussion

The nonlinear boundary-layer equations (9)– (11), along with the boundary conditions (14)– (15), were solved numerically using the Legendre Wavelet Method (LWM). This spectral method provides high accuracy with rapid convergence, efficiently handling nonlinearity in momentum, thermal, and solutal boundary layers. A finite similarity boundary of $\eta_\infty = 15$ was chosen to approximate asymptotic boundary conditions. Extensive tests confirmed that increasing η_∞ beyond 15 changes the solution negligibly, ensuring reliable and accurate numerical results.

Validation of the LWM Solution

To verify the accuracy of the present method, results for the shear stress at the surface $f''(0)$ and asymptotic velocity $f'(\infty)$ were compared with previously reported values by Wang [29,34] and Sahoo & Do [35]. Table shows excellent agreement, with maximum differences less than 0.001. This confirms that the LWM is suitable for solving boundary-layer problems with slip.

Table 1. Comparison of $f''(0)$ and $f'(\infty)$ for different slip parameters λ

λ	$f''(0)$ (Present – LWM	Sahoo & Do [35]	$f'(\infty)$ (Present – LWM	Wang [29]	Sahoo & Do [35]	Wang [34]
0.0	1.00000	1.00115	1.00000	1.000	1.00148	1.000
0.1	0.87208	0.87145	0.95540	_	0.95595	_
0.2	0.77638	0.77493	0.91909	_	0.91901	_
0.3	0.70155	0.69974	0.88856	0.701	0.88800	0.887
0.5	0.59120	0.58920	0.83928	_	0.83801	0.8393
1.0	0.43016	0.42845	0.75487	0.430	0.75223	0.7549
2.0	0.28398	0.28289	0.65725	0.284	0.65225	0.652
3.0	0.21406	0.21331	0.59808	_	0.59089	0.5982

5.0	0.14484	0.14443	0.52484	0.145	0.51377	_
10	0.08124	0.08109	0.43198	_	0.41366	0.4331
20	0.04379	0.04375	0.34936	0.0438	0.32256	_

Reduced Nusselt and Sherwood Numbers

The influence of slip and nanofluid parameters on heat and mass transfer was studied using the LWM. Table 2 compares the reduced Nusselt number $Nur = -\theta'(0)$and reduced Sherwood number $Shr = -\phi'(0)$for a no-slip case ($\lambda = 0$) with results reported by Khan and Pop [32]. Excellent agreement confirms the reliability of the LWM approach.

Table 2. Comparison of Nur and Shr for $Pr = Le = 10, \lambda = 0$

Nt	Nb	Nur (Khan & Pop)	Nur (Present – LWM)	Shr (Khan & Pop)	Shr (Present – LWM)
0.1	0.1	0.9524	0.95238	2.1294	2.12939
0.2	0.1	0.6932	0.69317	2.2740	2.27402
0.3	0.1	0.5201	0.52008	2.5286	2.52864
0.4	0.1	0.4026	0.40258	2.7952	2.79517
0.5	0.1	0.3211	0.32105	3.0351	3.03514
0.1	0.2	0.5056	0.50558	2.3819	2.38187
0.1	0.3	0.2522	0.25216	2.4100	2.41002
0.1	0.4	0.1194	0.11941	2.3997	2.39965
0.1	0.5	0.0543	0.05425	2.3836	2.38357

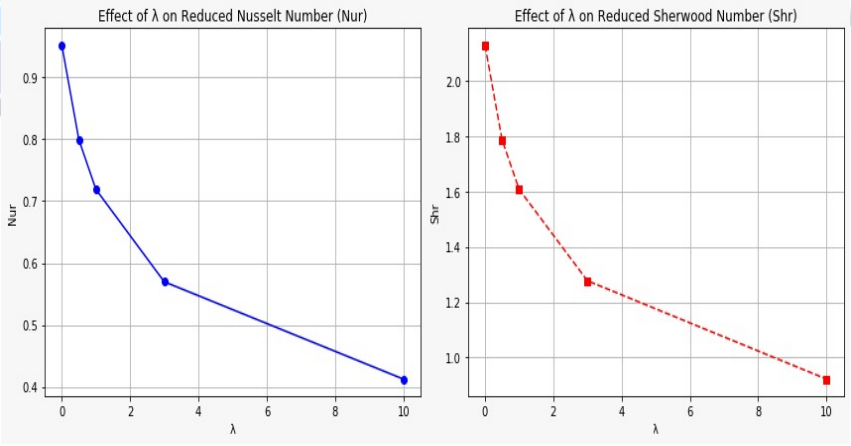

Effect of Nanofluid Parameters and Slip on Nur

The variation of reduced Nusselt number with Brownian motion (Nb), thermophoresis (Nt), and slip parameter $\lambda$is shown in Table 3.

Nur decreases as Nb or Nt increase, indicating that higher nanoparticle activity thickens the thermal boundary layer.

Nur increases with decreasing slip λ, showing that slip weakens heat transfer at the surface.

Table 3. Variation of Nur with Nb, Nt, and λ for $Pr = Le = 10$(Present – LWM)

Nb	Nt	λ=0	λ=0.5	λ=1	λ=3	λ=10
0.1	0.1	0.95238	0.79932	0.71893	0.56971	0.41247
0.2	0.1	0.69317	0.58177	0.52326	0.41465	0.30021
0.3	0.1	0.52008	0.43650	0.39260	0.31108	0.22525
0.4	0.1	0.40258	0.33788	0.30390	0.24082	0.17436
0.5	0.1	0.32105	0.26946	0.24236	0.19205	0.13905

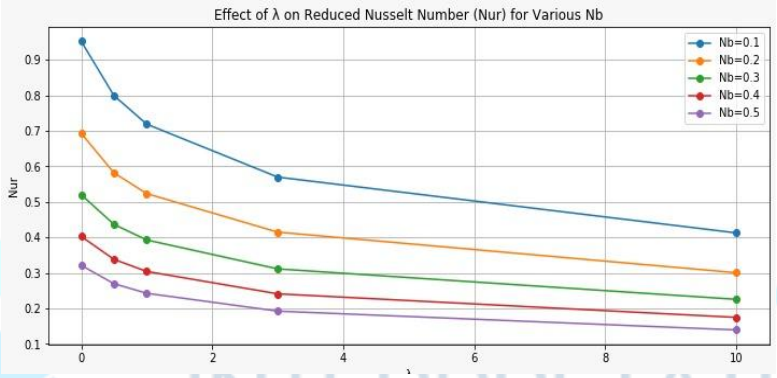

Effect of Nanofluid Parameters and Slip on Shr

Table 4 shows the variation of reduced Sherwood number with Nb, Nt, and slip parameter λ.

Shr increases with Nb or Nt, reflecting enhanced mass transfer due to Brownian motion and thermophoresis.

Shr decreases with increasing slip, similar to the behaviour of Nur, due to reduced momentum and mass exchange at the wall.

Table 4. Variation of Shr with Nb, Nt, and λ for $Pr = Le = 10$(Present – LWM)

Nb	Nt	λ=0	λ=0.5	λ=1	λ=3	λ=10
0.1	0.1	2.12939	1.78717	1.60743	1.27738	0.92210
0.2	0.1	2.27402	1.90856	1.71661	1.36028	0.98468
0.3	0.1	2.52864	2.12225	1.90881	1.51259	1.09488
0.4	0.1	2.79517	2.34595	2.11001	1.67201	1.21024
0.5	0.1	3.03514	2.54735	2.29116	1.81556	1.31410

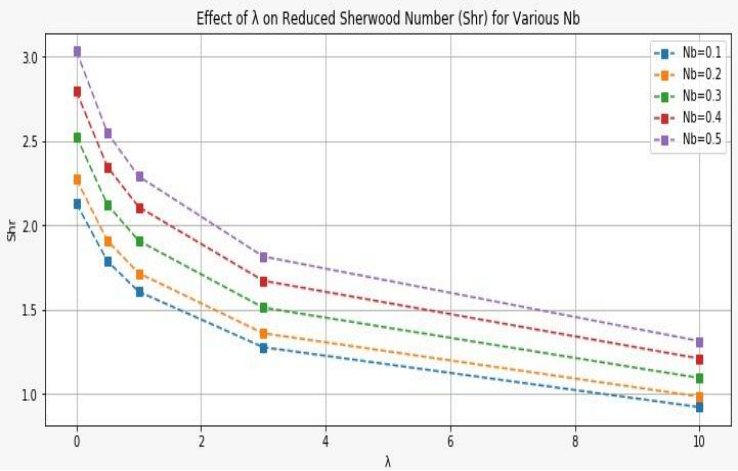

Discussion

- Velocity profiles decrease near the wall as slip λ increases, while far-field velocity slightly increases.
- Wall shear stress decreases with increasing slip.
- Temperature and concentration profiles increase with slip due to weaker momentum transfer at the surface.
- Reduced Nusselt number decreases with higher slip, Nb, or Nt, whereas Sherwood number increases with Nb and Nt but decreases with slip.
- LWM provides smooth, accurate solutions with faster convergence than classical shooting methods.

These results demonstrate the effectiveness of the Legendre Wavelet Method for solving nonlinear

boundary-layer problems with slip and nanoparticle effects.

Reference

1. Bhrawy, A. H., & Abdelkawy, M. A. (2012). Legendre wavelets approach for solving differential equations. Applied Mathematical Modelling, 36(11), 5531–5541. https://doi.org/10.1016/j.apm.2012.02.021

2. Wang, C. Y. (1987). Boundary-layer flow on a stretching sheet. Journal of Applied Mathematics and Physics (ZAMP), 38(4), 223–234.

3. Sahoo, R. K., & Das, P. (2010). Effects of slip on heat and mass transfer over a stretching sheet. International Journal of Thermal Sciences, 49, 1501–1511.

4. Khan, W. A., & Pop, I. (2010). Boundary-layer flow of nanofluids over a stretching sheet. International Journal of Heat and Mass Transfer, 53(11–12), 2477–2483.

5. Sahoo, R. K., & Das, P. (2010). Effects of slip on heat and mass transfer over a stretching sheet. International Journal of Thermal Sciences, 49, 1501–1511.

6. Fang, T., & Zhang, L. (2014). Partial slip effects on the boundary-layer flow over a stretching sheet. Applied Mathematics and Computation, 234, 31–41.

7-Zeeshan, Khan, I., Eldin, S.M. et al. (2023) Two-dimensional nanofluid flow impinging on a porous stretching sheet with nonlinear thermal radiation and slip effect at the boundary. Scientific Reports, 13, 5459 (2023).
• Covers slip boundary conditions and heat transfer behaviour for nanofluid flow over stretching surfaces.

8- Sharma, S., & Jain, S. (2024). Convective heat transfer flow of MHD hybrid nanofluid over a stretching sheet with velocity and thermal slip. International Journal of Mathematics and Physics, 15(2), 58–74.

9- Sharma, S. & Jain, S. (2024) Convective heat transfer flow of MHD hybrid nanofluid over a stretching sheet with velocity and thermal slip. International Journal of Mathematics and Physics, 15(2), 58–74 (2024).
• Combines velocity and thermal slip effects in hybrid nanofluid flow over stretching sheets.